JACS
JOURNAL OF THE AMERICAN CHEMICAL SOCIETY

Subscriber access provided by American Chemical Society

Article

Mechanisms of Hydrogen-, Oxygen-, and Electron-Transfer Reactions of Cumylperoxyl Radical

Shunichi Fukuzumi, Kanji Shimoosako, Tomoyoshi Suenobu, and Yoshihito Watanabe

J. Am. Chem. Soc., **2003**, 125 (30), 9074-9082• DOI: 10.1021/ja035156o • Publication Date (Web): 02 July 2003

Downloaded from http://pubs.acs.org on March 29, 2009

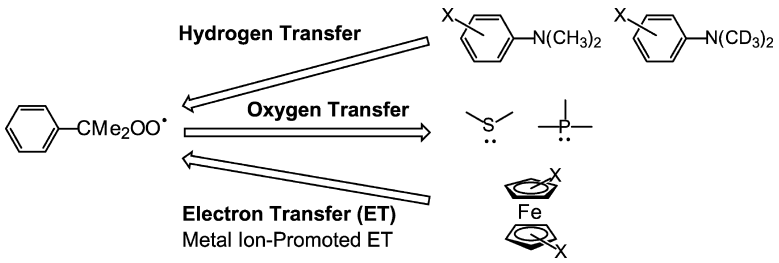

More About This Article

Additional resources and features associated with this article are available within the HTML version:

- Supporting Information
- Links to the 7 articles that cite this article, as of the time of this article download
- Access to high resolution figures
- Links to articles and content related to this article
- Copyright permission to reproduce figures and/or text from this article

View the Full Text HTML

ACS Publications
High quality. High impact.

Journal of the American Chemical Society is published by the American Chemical Society. 1155 Sixteenth Street N.W., Washington, DC 20036

J|A|C|S
ARTICLES
Published on Web 07/02/2003

Mechanisms of Hydrogen-, Oxygen-, and Electron-Transfer Reactions of Cumylperoxyl Radical

Shunichi Fukuzumi,*,† Kanji Shimoosako,† Tomoyoshi Suenobu,† and Yoshihito Watanabe‡

Contribution from the Department of Material and Life Science, Graduate School of Engineering, Osaka University, CREST, Japan Science and Technology Corporation (JST), Suita, Osaka 565-0871, Japan, and Department of Chemistry, Graduate School of Science, Nagoya University, Chikusa-ku, Nagoya 464-8602, Japan

Received March 14, 2003; E-mail: fukuzumi@chem.eng.osaka-u.ac.jp

Abstract: Rates of hydrogen-transfer reactions from a series of *para*-substituted *N*,*N*-dimethylanilines to cumylperoxyl radical and oxygen-transfer reactions from cumylperoxyl radical to a series of sulfides and phosphines have been determined in propionitrile (EtCN) and pentane at low temperatures by use of ESR. The observed rate constants exhibit first-order and second-order dependence with respect to concentrations of *N*,*N*-dimethylanilines. This indicates that the hydrogen- and oxygen-transfer reactions proceed via 1:1 charge-transfer (CT) complexes formed between the substrates and cumylperoxyl radical. The primary kinetic isotope effects are determined by comparing the rates of *N*,*N*-dimethylanilines and the corresponding *N*,*N*-bis(trideuteriomethyl)anilines. The isotope effect profiles are quite different from those reported for the P-450 model oxidation of the same series of substrates. Rates of electron-transfer reactions from ferrocene derivatives to cumylperoxyl radical have also been determined by use of ESR. The catalytic effects of $Sc(OTf)_3$ (OTf = triflate) on the electron-transfer reactions are compared with those of $Sc(OTf)_3$ on the hydrogen- and oxygen-transfer reactions. Such comparison provides strong evidence that the hydrogen- and oxygen- transfer reactions of cumylperoxyl radical proceed via a one-step hydrogen atom and oxygen atom transfer rather than via an electron transfer from substrates to cumylperoxyl radical.

Introduction

Hydrogen transfer is a common mechanism of organic free radical chemistry, playing an important role in the oxidation and halogenation of hydrocarbons[1] and also in enzymatic oxidation.[2] The hydrogen-transfer reactions from amines to alkoxyl[3] and peroxyl radicals[4] have attracted special attention in relation to the enzymatic mechanism for the oxidative dealkylation of amines by cytochrome P-450.[5−11] There are two possibilities in the mechanisms of the hydrogen-transfer reactions, i.e., a one-step hydrogen atom transfer or electron transfer followed by proton transfer.[5−12] The mechanism of oxygen-transfer reactions from the active oxygen intermediates of P-450 to versatile organic compounds such as sulfides and phosphines has also been studied extensively.[11,13,14] In the case of oxygen-transfer reactions as well, a mechanistic dichotomy whether the oxygen transfer occurs via a one-step direct oxygen atom transfer or via electron transfer has been discussed.[14] In this context, we have previously reported that the effects of metal ions provide a reliable criterion for distinguishing between the one-step hydrogen-transfer and electron-transfer mechanisms in

† Osaka University.
‡ Nagoya University.

(1) (a) *Free Radicals*; Kochi, J. K. Ed.; Wiley: New York, 1973. (b) Perkins, M. J. *Free Radical Chemistry*; Ellis Horwood: New York, 1994.
(2) (a) Hawkins, C. L.; Davies, M. J. *Biochim. Biophys. Acta* **2001**, *1504*, 196. (b) Jordan, A.; Reichard, P. *Annu. Rev. Biochem.* **1998**, *67*, 71. (c) Whittaker, J. W. *Adv. Protein Chem.* **2002**, *60*, 1. (d) Itoh, S.; Taki, M.; Fukuzumi, S. *Coord. Chem. Rev.* **2000**, *198*, 3. (e) Chaudhuri, P.; Wieghardt, K. *Prog. Inorg. Chem.* **2001**, *50*, 151.
(3) (a) Paul, H.; Small, R. D., Jr.; Scaiano, J. C. *J. Am. Chem. Soc.* **1978**, *100*, 4520. (b) Griller, D.; Howard, J. A.; Marriott, P. R.; Scaiano, J. C. *J. Am. Chem. Soc.* **1981**, *103*, 619. (b) Encina, M. V.; Lissi, E. A. *Int. J. Chem. Kinet.* **1978**, *10*, 653.
(4) Howard, J. A. *Adv. Free-Radical Chem. (London)* **1972**, *4*, 49.
(5) (a) Karki, S. B.; Dinnocenzo, J. P.; Jones, J. P.; Korzekwa, K. R. *J. Am. Chem. Soc.* **1995**, *117*, 3657. (b) Manchester, J. I.; Dinnocenzo, J. P.; Higgins, L. A.; Jones, J. P. *J. Am. Chem. Soc.* **1997**, *119*, 5069.
(6) (a) Shaffer, C. L.; Morton, M. D.; Hanzlik, R. P. *J. Am. Chem. Soc.* **2001**, *123*, 8502. (b) Shaffer, C. L.; Harriman, S.; Koen, Y. M.; Hanzlik, R. P. *J. Am. Chem. Soc.* **2002**, *124*, 8268.
(7) (a) Guengerich, F. P.; Macdoland, T. L. In *Advances in Electron-Transfer Chemistry*; Mariano, P. S., Ed.; JAI Press: Greenwich, 1993; Vol. 3, pp 191−241. (b) Sato, H.; Guengerich, F. P. *J. Am. Chem. Soc.* **2000**, *122*, 8099. (c) Guengerich, F. P.; Yun, C.-H.; Macdonald, T. L. *J. Biol. Chem.* **1996**, *271*, 27321.
(8) Bhakta, M. N.; Wimalasena, K. *J. Am. Chem. Soc.* **2002**, *124*, 1844.
(9) (a) Wright, J. S.; Johnson, E. R.; DiLabio, G. A. *J. Am. Chem. Soc.* **2001**, *123*, 1173. (b) Migliavacca, E.; Carrupt, P.-A.; Testa, B. *Helv. Chim. Acta* **1997**, *80*, 1613.
(10) Goto, Y.; Watanabe, Y.; Fukuzumi, S.; Jones, J. P.; Dinnocenzo, J. P. *J. Am. Chem. Soc.* **1998**, *120*, 10762.
(11) Ortiz de Montellano, P. R. *Cytochrome P450. Structure, Mechanism, and Biochemistry*, 2nd ed.; Plenum Publishing Corporation: New York, 1995.
(12) When an electron and a proton are transferred in a single step, there are also two mechanisms: hydrogen atom transfer and proton-coupled electron transfer. The precise definition of proton-coupled electron transfer has yet to be widely accepted, but this term is often applied to mechanisms in which the proton and electron are transferred between different sets of orbitals. See: (a) Cukier, R. I.; Nocera, D. G. *Annu. Rev. Phys. Chem.* **1998**, *49*, 337. (b) Kohen, A.; Klinman, J. P. *Acc. Chem. Res.* **1998,** *31*, 397. (c) Hammes-Schiffer, S. *Acc. Chem. Res.* **2001**, *34*, 273. (d) Mayer, J. M.; Hrovat, D. A.; Thomas, J. L.; Borden, W. T. *J. Am. Chem. Soc.* **2002**, *124*, 11142.
(13) (a) Guengerich, F. P.; Macdonald, T. L. *Acc. Chem. Res.* **1984**, *17*, 9. (b) Guengerich, F. P.; Shimada, T. *Chem. Res. Toxicol.* **1991**, *4*, 391.
(14) Goto, Y.; Matui, T.; Ozaki, S.; Watanabe, Y.; Fukuzumi, S. *J. Am. Chem. Soc.* **1999**, *121*, 9497.

10.1021/ja035156o CCC: $25.00 **© 2003 American Chemical Society**

hydrogen-transfer reactions of radical species.[15] However, there has been no report on the effects of metal ions on the electron-transfer reactions of alkoxyl and peroxyl radicals. Direct measurements of the rates of alkoxyl radicals by ESR have not been possible because of the extremely short lifetimes of the radicals.[16]

We report herein comprehensive studies on determination of the absolute rates of hydrogen-transfer reactions from a series of *para*-substituted *N*,*N*-dimethylanilines to cumylperoxyl radical and those of oxygen transfer from cumylperoxyl radical to sulfides and phosphines by use of ESR at low temperatures. Cumylperoxyl radical, while much less reactive than alkoxyl radicals, is known to follow the same pattern of relative reactivity with a variety of substrates.[17,18] The detailed kinetic study provides valuable insight into the hydrogen- and oxygen-transfer mechanisms. Electron-transfer rates from ferrocene derivatives to cumylperoxyl radical have also been determined for the first time at low temperatures by ESR. The resulting data are evaluated in light of the Marcus theory of electron transfer[19] to determine the reorganization energy of electron transfer of cumylperoxyl radical. The effects of metal ions on the electron-, hydrogen-, and oxygen-transfer reactions of cumylperoxyl radical are compared in order to distinguish between a one-step hydrogen atom or oxygen atom transfer mechanism and an electron-transfer mechanism.

Experimental Section

Materials. Di-*tert*-butyl peroxide was purchased from Nacalai Tesque Co., Ltd. and purified by chromatography through alumina, which removes traces of the hydroperoxide. Cumene was purchased from Tokyo Kasei Co., Ltd. *para*-Substituted *N*,*N*-dimethylanilines (DMAs) [*N*,*N*-dimethylaniline, DMA; *p*-methoxy-*N*,*N*-dimethylaniline, MeO-DMA; *p*-methyl-*N*,*N*-dimethylaniline, Me-DMA; *p*-bromo-*N*,*N*-dimethylaniline, Br-DMA; *p*-cyano-*N*,*N*-dimethylaniline, CN-DMA] were also commercially available and purified by the standard procedure.[20] Deuterated compounds [*N*,*N*-bis(trideuteriomethyl)aniline, DMA-$(CD_3)_2$; *p*-methyl-*N*,*N*-bis(trideuteriomethyl)aniline, Me-DMA-$(CD_3)_2$; *p*-methoxy-*N*,*N*-bis(trideuteriomethyl)aniline, MeO-DMA-$(CD_3)_2$] were prepared according to the literature.[21] *para*-Substituted thioanisole derivatives [thioanisole, TA; *p*-methoxythioanisole, MeO-TA; *p*-methylthioanisole, Me-TA; *p*-chlorothioanisole, Cl-TA], dialkyl sulfides, diphenyl sulfide, and phosphines were purchased from Aldrich Co., Ltd. or Tokyo Kasei Co., Ltd. Ferrocene derivatives were purchased from Aldrich Co., Ltd. Pentane and propionitrile (EtCN) used as solvents were purified and dried by the standard procedure.[20]

Kinetic Measurements. Kinetic measurements were performed on a JEOL X-band ESR spectrometer (JES-ME-LX) at low temperatures (193−233 K). Typically, photoirradiation of an oxygen-saturated propionitrile solution containing di-*tert*-butyl peroxide (1.0 M) and cumene (1.0 M) with a 1000-W mercury lamp resulted in formation of cumylperoxyl radical ($g = 2.0156$), which could be detected at low temperatures. The g value was calibrated by using an Mn^{2+} marker. Upon cutoff of the light, the decay of the ESR intensity was recorded with time. The decay rate was accelerated by the presence of DMA (1.0×10^{-2} M). Rates of hydrogen transfer from *para*-substituted *N*,*N*-dimethylanilines (DMAs) to $PhCMe_2OO^\bullet$ were monitored by measuring the decay of ESR signal of $PhCMe_2OO^\bullet$ in the presence of various concentrations of DMAs in EtCN and pentane at 193 K. Pseudo-first-order rate constants were determined by a least-squares curve fit using a Macintosh personal computer. The first-order plots of $\ln(I - I_\infty)$ versus time (I and I_∞ are the ESR intensity at time t and the final intensity, respectively) were linear for three or more half-lives with the correlation coefficient $\rho > 0.99$. In each case, it was confirmed that the rate constants determined from at least five independent measurements agreed within an experimental error of ±5%. The primary kinetic isotope effects were determined by determining the rates of hydrogen transfer from DMA or DMA-$(CD_3)_2$ to $PhCMe_2OO^\bullet$ at various temperatures. Rates of electron transfer from ferrocene derivatives to $PhCMe_2OO^\bullet$ were also monitored by measuring the decay of ESR signal of $PhCMe_2OO^\bullet$ in the presence of various concentrations of ferrocene derivatives in EtCN at 193 K. The effects of metal ions on the electron-transfer reactions were examined by determining the decay rates of $PhCMe_2OO^\bullet$ in the presence of ferrocene derivatives and metal ions.

Reaction Procedure. Typically, triphenylphosphine (Ph_3P) (7.0×10^{-2} M) was added to the 1-cm UV cell that contained an O_2-saturated CD_3CN solution of di-*tert*-butyl peroxide (1.0×10^{-1} M) and cumene (1.0×10^{-1} M) at room temperature and was photoirradiated for 15 min. After photoirradiation, the product was identified as triphenylphosphine oxide ($Ph_3P{=}O$) by comparing the ^1H NMR spectra with those of authentic samples. The ^1H NMR measurements were performed with Japan Electron Optics JNM-GSX-400 (400 MHz) NMR spectrometers. ^1H NMR (CD_3CN, 298 K) δ (Me_4Si, ppm): $Ph_3P{=}O$ δ 7.5−7.7 (m, 15H); $MePhS{=}O$ δ 2.7 (s, 3H), 7.5−7.7 (m, 5H).

Electrochemical Measurements. Cyclic voltammetry (CV) measurements of DMAs, sulfides, and phosphines were performed on a BAS 100B electrochemical analyzer in deaerated MeCN containing 0.10 M n-$Bu_4N^+PF_6^-$ ($TBAPF_6$) as a supporting electrolyte at 298 K. The CV of $PhCMe_2OO^\bullet$ was measured in deaerated EtCN containing 0.10 M $TBAPF_6$ as a supporting electrolyte, $PhCMe_2OOH$ (2.0 mM), and n-Bu_4NOH (2.0 mM) as a base at 198 K. The second harmonic ac voltammetry (SHACV)[22] measurements of sulfides and phosphines were also performed on a BAS 100B electrochemical analyzer in deaerated MeCN containing 0.10 M $TBAPF_6$ as a supporting electrolyte at 298 K. The platinum working electrode was polished with BAS polishing alumina suspension and rinsed with acetone before use. The counter electrode was a platinum wire. The measured potentials were recorded with respect to an $Ag/AgNO_3$ (0.01 M) reference electrode. The E^0_{ox} values (vs Ag/Ag^+) are converted to those vs SCE by adding 0.29 V.[23]

Theoretical Calculations. The theoretical studies were performed using the PM3 molecular orbital method.[24] The calculations were performed by using the MOL-MOLIS program ver. 2.8 by Daikin Industries, Ltd. Final geometries and energetics were obtained by optimizing the total molecular energy with respect to all structural variables. The geometries of the radicals were optimized using the unrestricted Hartree−Fock (UHF) formalism. The ΔH_f values of the radicals were calculated with the UHF-optimized structures using the half-electron (HE) method with the restricted Hartree−Fock (RHF) formalism.[25] Density-functional theory (DFT) calculations were per-

(15) (a) Fukuzumi, S.; Tokuda, Y.; Chiba, Y.; Greci, L.; Carloni, P.; Damiani, E. *J. Chem. Soc., Chem. Commun.* **1993**, 1575. (b) Nakanishi, I.; Miyazaki, K.; Shimada, T.; Ohkubo, K.; Urano, S.; Ikota, N.; Ozawa, T.; Fukuzumi, S.; Fukuhara, K. *J. Phys. Chem. A* **2002**, *106*, 11123.
(16) (a) Ingold, K. U.; Morton, J. R. *J. Am. Chem. Soc*. **1964**, *86*, 3400. (b) Small, R. D., Jr.; Scaiano, J. C. *J. Am. Chem. Soc*. **1978**, *100*, 296.
(17) (a) Russell, G. A. *Free Radicals*; Kochi, J. K., Ed.; Wiley & Sons: New York, 1973; Chapter 7. (b) Russell, G. A. *J. Am Chem. Soc*. **1956**, *78*, 1047.
(18) Howard, J. A.; Ingold, K. U.; Symonds, M. *Can. J. Chem.* **1968**, *46*, 1017.
(19) (a) Marcus, R. A.; Eyring, H. *Annu. Rev. Phys. Chem*. **1964**, *15*, 155. (b) Marcus, R. A. *Angew. Chem., Int. Ed. Engl*. **1993**, *32*, 1111.
(20) Perrin, D. D.; Armarego, W. L. F. *Purification of Laboratory Chemicals;* Butterworth-Heinemann: Oxford, 1998.
(21) Dinnocenzo, J. P.; Karki, S. B.; Jones, J. P. *J. Am Chem. Soc*. **1993**, *115*, 7111.
(22) The SHACV method provides a superior approach for directly evaluating the one-electron redox potentials in the presence of a follow-up chemical reaction, relative to the better-known dc and fundamental harmonic ac methods: (a) Bond, A. M.; Smith, D. E. *Anal. Chem.* **1974**, *46*, 1946. (b) Arnett, E. M.; Amarnath, K.; Harvey, N. G.; Cheng, J.-P. *J. Am. Chem. Soc.* **1990**, *112*, 344.
(23) Mann, C. K.; Barnes, K. K. *Electrochemical Reactions in Nonaqueous Systems*; Marcel Dekker: New York, 1970.
(24) Stewart, J. J. P. *J. Comput. Chem*. **1989**, *10*, 209, 221.
(25) Clark, T. *A Handbook of Computational Chemistry*; Wiley: New York, 1985; p 97.

formed on a COMPAQ DS20E computer. Geometry optimizations were carried out using the B3LYP functional and 6-31G* basis set[26,27] as implemented in the Gaussian 98 program.[28] The geometries of the radicals were optimized using the unrestricted Hartree−Fock (UHF) formalism. At the stationary point a vibrational frequency analysis was performed to calculate the contribution of the zero-point vibrational energy (ZPE). The ZPEs from these frequency calculations were scaled by a factor of 0.980 to correct for the anharmonicity in the vibrational potential energy surface, the limited basis set, and the missing correlation effects.[29,30] The enthalpy changes of the hydrogen-transfer reactions ($\Delta\Delta H_f$) were calculated from the difference in the ZPE corrected total energies of each reactants and products according to the literature.[31]

Results and Discussion

Hydrogen Transfer from DMAs to Cumylperoxyl Radical. Direct measurements of the rates of hydrogen transfer from a series of *para*-substituted *N*,*N*-dimethylanilines (DMAs) to cumylperoxyl radical were performed in propionitrile (EtCN) at various temperatures by means of ESR. The photoirradiation of an oxygen-saturated EtCN solution containing di-*tert*-butylperoxide (Bu^tOOBu^t) and cumene with a 1000-W mercury lamp results in formation of cumylperoxyl radical, which was readily detected by ESR as shown in Figure 1. The cumylperoxyl radical is formed via a radical chain process shown in Scheme 1.[32,33] The photoirradiation of Bu^tOOBu^t results in the homolytic cleavage of the O−O bond to produce $Bu^tO^•$,[34,35] which abstracts a hydrogen from cumene to give cumyl radical, followed by the facile addition of oxygen to cumyl radical. The cumylperoxyl radical can also abstract a hydrogen atom from cumene in the propagation step to yield cumene hydroperoxide, accompanied by regeneration of cumyl radical (Scheme 1).[36] In the termination step, cumylperoxyl radicals decay by a bimolecular reaction to yield the corresponding peroxide and oxygen (Scheme 1).[4] When the light is cut off, the ESR signal intensity decays obeying second-order kinetics due to the bimolecular reaction in Scheme 1 as shown in Figure 1 (see the inset for the second-order plot for the decay of the ESR intensity of cumylperoxyl radicals).[4]

In the presence of DMA, the decay rate of cumylperoxyl radical after cutting off the light becomes much faster than that in the absence of DMA as shown in Figure 2. The decay rate in the presence of DMA (1.0×10^{-2} M) obeys pseudo-first-order kinetics rather than second-order kinetics (see the inset of Figure 2 for the first-order plot). Thus, this decay process is

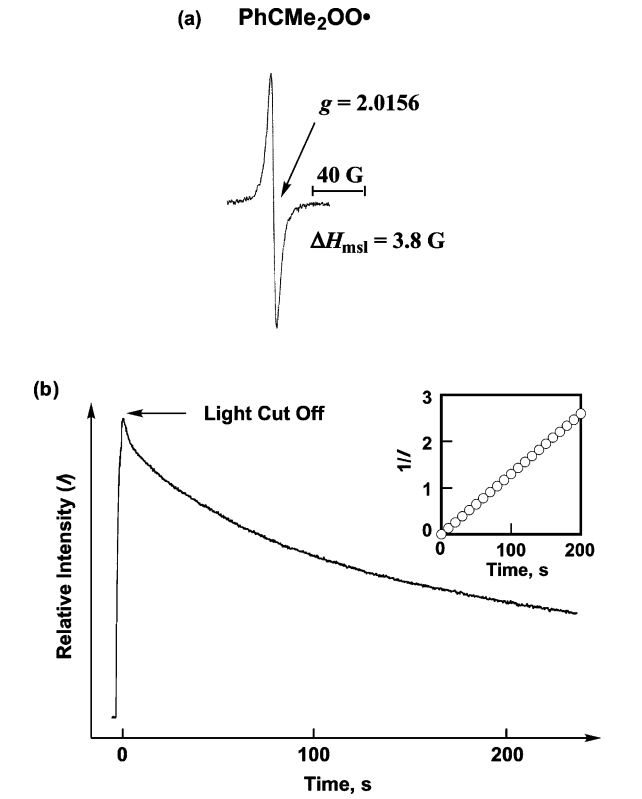

Figure 1. (a) ESR signal observed in photolysis of an O_2-saturated EtCN solution of di-*tert*-butyl peroxide (1.0 M) and cumene (1.0 M) with a 1000-W mercury lamp at 193 K. (b) The decay profile of the ESR intensity upon cutting off the light in O_2-saturated EtCN at 193 K. Inset: second-order plot.

Scheme 1

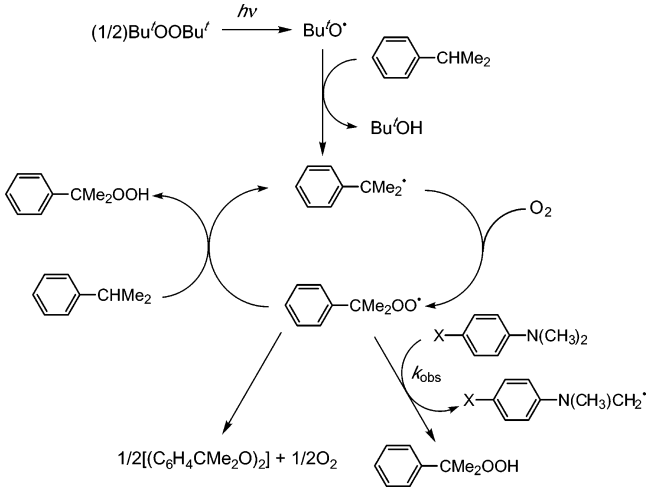

(26) (a) Becke, A. D. *J. Chem. Phys.* **1993**, *98*, 5648. (b) Lee, C.; Yang, W.; Parr, R. G. *Phys. Rev. B* **1988**, *37*, 785.
(27) Hehre, W. J.; Radom, L.; Schleyer, P. v. R.; Pople, J. A. *Ab Initio Molecular Orbital Theory*; Wiley: New York, 1986.
(28) Frisch, M. J.; Trucks, G. W.; Schlegel, H. B.; Scuseria, G. E.; Robb, M. A.; Cheeseman, J. R.; Zakrzewski, V. G.; Montgomery, J. A., Jr.; Stratmann, R. E.; Burant, J. C.; Dapprich, S.; Millam, J. M.; Daniels, A. D.; Kudin, K. N.; Strain, M. C.; Farkas, O.; Tomasi, J.; Barone, V.; Cossi, M.; Cammi, R.; Mennucci, B.; Pomelli, C.; Adamo, C.; Clifford, S.; Ochterski, J.; Petersson, G. A.; Ayala, P. Y.; Cui, Q.; Morokuma, K.; Malick, D. K.; Rabuck, A. D.; Raghavachari, K.; Foresman, J. B.; Cioslowski, J.; Ortiz, J. V.; Baboul, A. G.; Stefanov, B. B.; Liu, G.; Liashenko, A.; Piskorz, P.; Komaromi, I.; Gomperts, R.; Martin, R. L.; Fox, D. J.; Keith, T.; Al-Laham, M. A.; Peng, C. Y.; Nanayakkara, A.; Gonzalez, C.; Challacombe, M.; Gill, P. M. W.; Johnson, B.; Chen, W.; Wong, M. W.; Andres, J. L.; Gonzalez, C.; Head-Gordon, M.; Replogle, E. S.; Pople, J. A. *Gaussian 98*, revision A.7; Gaussian, Inc.: Pittsburgh, PA, 1998.
(29) (a) Wong, M. W.; Pross, A.; Radom, L. *J. Am. Chem. Soc.* **1993**, *115*, 11050. (b) Wong, M. W. *Chem. Phys. Lett.* **1996**, *256*, 391. (c) Scott, A. P.; Radom, L. *J. Phys. Chem.* **1996**, *100*, 16502.
(30) (a) Bauschlicher, C. W., Jr.; Partridge, H. *J. Chem. Phys.* **1995**, *103*, 1788. (b) Pople, J. A.; Scott, A. P.; Wong, M. W.; Radom, L. *Isr. J. Chem.* **1993**, *33*, 345.
(31) Fox, T.; Kollman, P. A. *J. Phys. Chem.* **1996**, *100*, 2950.
(32) (a) Sheldon, R. A. In *The Activation of Dioxygen and Homogeneous Catalytic Oxidation*; Barton, D. H. R., Martell, A. E., Sawyer, D. T., Eds.; Plenum: New York and London, 1933; pp 9−30. (b) Parshall, G. W.; Ittel, S. D. *Homogeneous Catalysis*, 2nd ed.; Wiley: New York, 1992; Chapter 10. (c) Sheldon, R. A.; Kochi, J. K. *Adv. Catal.* **1976**, *25*, 272.
(33) (a) Shilov, A. E. *Activation of Saturated Hydrocarbons by Transition Metal Complexes*; D. Reidel Publishing Co.: Dordrecht, The Netherlands, 1984; Chapter 4. (b) Boettcher, A.; Birnbaum, E. R.; Day, M. W.; Gray, H. B.; Grinstaff, M. W.; Labinger, J. A. *J. Mol. Catal. A* **1997**, *117*, 229.
(34) Kochi, J. K. *Free Radicals in Solution*; J. Wiley & Sons: New York, 1957.
(35) (a) Kochi, J. K.; Krusic, P. J.; Eaton, D. R. *J. Am. Chem. Soc.* **1969**, *91*, 1877. (b) Krusic, P. J.; Kochi, J. K. *J. Am. Chem. Soc.* **1968**, *90*, 7155. (c) Krusic, P. J.; Kochi, J. K. *J. Am. Chem. Soc.* **1969**, *91*, 3938. (d) Krusic, P. J.; Kochi, J. K. *J. Am. Chem. Soc.* **1969**, *91*, 3942. (e) Kochi, J. K.; Krusic, P. J. *J. Am. Chem. Soc.* **1969**, *91*, 3944. (f) Howard, J. A.; Furimsky, E. *Can. J. Chem.* **1974**, *52*, 555.
(36) (a) Fukuzumi, S.; Ono, Y. *J. Chem. Soc., Perkin Trans. 2* **1977**, 622. (b) Fukuzumi, S.; Ono, Y. *J. Chem. Soc., Perkin Trans. 2* **1977**, 784.

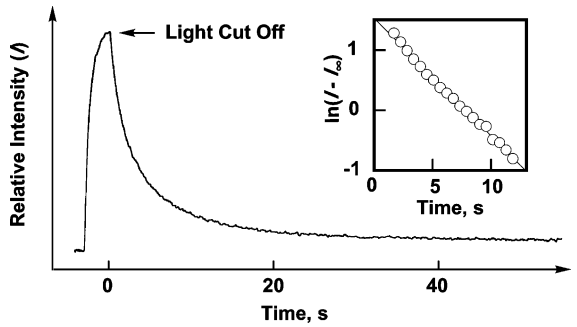

Figure 2. The decay profile of the ESR signal intensity due to $PhCMe_2OO^{\bullet}$ in the presence of DMA (1.0×10^{-2} M) in O_2-saturated EtCN at 193 K. Inset: pseudo-first-order plot.

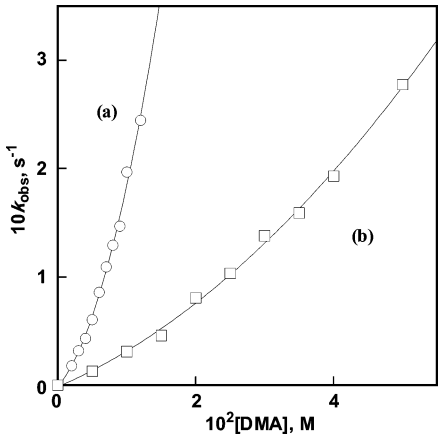

Figure 3. Plots of (a) k_{obs} versus [DMA] and (b) k_{obs} versus [DMA-$(CD_3)_2$] for hydrogen transfer from DMA and DMA-$(CD_3)_2$ to $PhCMe_2OO^{\bullet}$ in O_2-saturated EtCN at 193 K.

ascribed to the hydrogen transfer from DMA to cumylperoxyl radical (Scheme 1). The pseudo-first-order rate constants (k_{obs}) increase with an increase in [DMA] to exhibit first-order dependence on [DMA] at low concentrations, changing to second-order dependence at high concentrations as shown in Figure 3a. Such a first-order and second-order dependence of k_{obs} on substrate concentration is often observed in a variety of electrophilic reactions such as bromination of electron donors (olefins, alkylbenzenes and organometals), which proceeds via charge-transfer complexes formed between electron donors and electrophiles.[37] The mechanistic insight of the first-order and second-order dependence of k_{obs} on [DMA] will be discussed in detail later.

A similar dependence of k_{obs} on the concentration of a hydrogen donor is obtained when DMA is replaced by *N*,*N*-bis(trideuteriomethyl)aniline (DMA-$(CD_3)_2$) as shown in Figure 3b. The k_{obs} value of DMA-$(CD_3)_2$ is much smaller than that of DMA, indicating that there is a large primary kinetic isotope effect (k_H/k_D). The k_H/k_D value increases with increasing the DMA or DMA-$(CD_3)_2$ concentration. Arrhenius plots of the k_{obs} values for DMA and DMA-$(CD_3)_2$ at a constant DMA or DMA-$(CD_3)_2$ concentration (5.0×10^{-3} M) are shown in Figure 4, which indicates that the apparent k_H/k_D value decreases significantly with increasing temperature (e.g., $k_H/k_D = 4.2$ at 193 K and $k_H/k_D = 1.7$ at 233 K).

(37) Fukuzumi, S.; Kochi, J. K. *Int. J. Chem. Kinet.* **1983**, *15*, 249 and references therein.

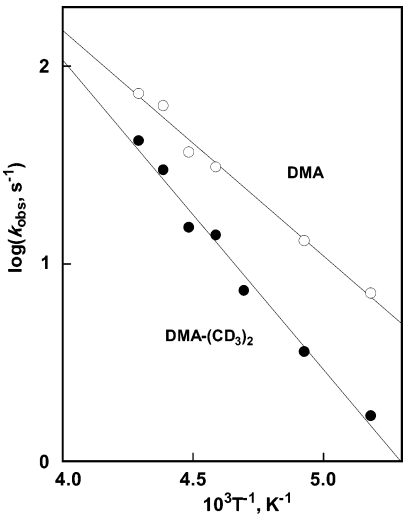

Figure 4. Arrhenius plots of k_{obs} for hydrogen transfer from DMA and DMA-$(CD_3)_2$ to $PhCMe_2OO^{\bullet}$ in O_2-saturated EtCN.

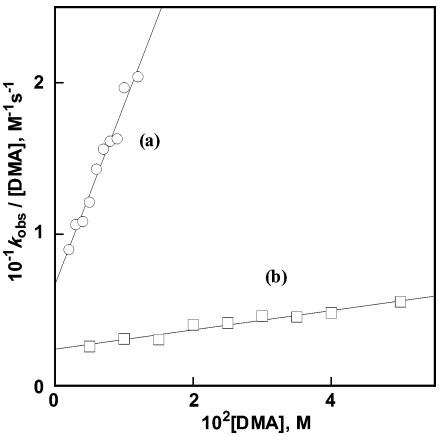

Figure 5. Plots of (a) k_{obs}/[DMA] versus [DMA] and (b) k_{obs}/[DMA-$(CD_3)_2$] versus [DMA-$(CD_3)_2$] for hydrogen transfer from DMA or DMA-$(CD_3)_2$ to $PhCMe_2OO^{\bullet}$ in O_2-saturated EtCN at 193 K.

The first-order and second-order dependence of k_{obs} on [DMA] can be separated by a linear correlation between k_{obs}/[DMA] and [DMA] as given by eq 1. The linear plot of

$$\frac{k_{obs}}{[DMA]} = k_1 + k_2[DMA] \qquad (1)$$

k_{obs}/[DMA] versus [DMA] is shown in Figure 5a together with the corresponding plot for DMA-$(CD_3)_2$ (Figure 5b). From the slopes and intercepts are obtained the k_1 and k_2 values. The primary kinetic isotope effect for the first-order dependence ($k_1^H/k_1^D = 2.8$) is much smaller than that for the second-order dependence ($k_2^H/k_2^D = 15$). This is the reason the apparent k_{obs}^H/k_{obs}^D values vary depending on the DMA and DMA-$(CD_3)_2$ concentrations and temperature.[38] Similar linear plots were obtained for hydrogen-transfer reactions from a series of DMAs and the deuterated compounds to cumylperoxyl radical in EtCN and pentane at 193 K (see Supporting Information S1). The k_1 and k_2 values thus determined are summarized in Table 1

(38) The different primary kinetic isotope effects ($k_1^H/k_1^D = 2.8$ and $k_2^H/k_2^D = 15$) in Figure 5 indicate involvement of different species in the hydrogen-transfer reaction. The large k_2^H/k_2^D value indicates the contribution of tunneling, but the reason of the difference from the k_1^H/k_1^D value has yet to be clarified.

Table 1. Oxidation Potentials and Rate Constants (k_1, k_2) for Hydrogen Transfer from *para*-Substituted DMA to $PhCMe_2OO^•$ in O_2-Saturated EtCN and Pentane at 193 K

p-substituted DMA	E^0_{ox} (vs SCE,[a] V)	k_1[b] ($M^{-1}\,s^{-1}$)	k_2[b] ($M^{-2}\,s^{-1}$)
MeO-DMA	0.52	4.9 (4.3)[c]	1.2×10^3 (1.2×10^3)[c]
MeO-DMA-$(CD_3)_2$	0.52	4.4 (1.2)[c]	1.2×10^3 (1.1×10^3)[c]
Me-DMA	0.69	3.2 (3.2)[c]	1.4×10^3 (2.0×10^3)[c]
Me-DMA-$(CD_3)_2$	0.69	2.4 (2.7)[c]	1.0×10^3 (1.9×10^2)[c]
DMA	0.76	6.7 (5.1)[c]	9.6×10^2 (5.0×10^2)[c]
DMA-$(CD_3)_2$	0.76	2.4 (0.7)[c]	6.4×10 (8.0×10)[c]
Br-DMA	0.92	1.9	6.0×10
CN-DMA	1.15	5.0×10^{-1}	9.0

[a] Determined in MeCN. [b] Determined in EtCN. [c] Values in parentheses are determined in pentane.

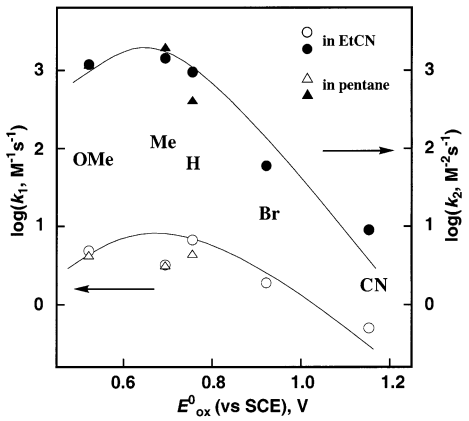

Figure 6. Plots of log k_1 and log k_2 versus E^0_{ox} of DMAs for hydrogen transfer from DMAs to $PhCMe_2OO^•$ in O_2-saturated EtCN and pentane at 193 K.

together with the one-electron oxidation potentials of DMAs (E^0_{ox}), which were determined by the cyclic voltammetry measurements (see Experimental Section).[39]

The dependence of log k_1 and log k_2 on E^0_{ox} is shown in Figure 6. The k_1 and k_2 values increase with decreasing E^0_{ox} but they decrease slightly through the maximum values at the lower E^0_{ox} values. Such a bell-shaped type dependence of k_1 and k_2 on E^0_{ox} is inconsistent with an electron-transfer mechanism, since the rate of electron transfer would increase with decreasing the E^0_{ox} value as the electron transfer becomes thermodynamically more favorable. The similar k_1 and k_2 values in a polar solvent (EtCN) and a nonpolar solvent (pentane) in Table 1 suggest that the hydrogen transfer from DMAs to cumylperoxyl radical proceeds via a one-step hydrogen atom transfer rather than sequential transfer of electron and proton. If this is the case, the k_1 and k_2 values may be correlated with the enthalpy change of the hydrogen-transfer reactions. The difference in heat of formation ($\Delta\Delta H_f$) between DMAs and the hydrogen-abstracted radicals DMA(−H)s is calculated by using the PM3 semiempirical MO method (see Experimental Section). The substituent effects of electron-donating or electron-withdrawing groups of DMAs on the $\Delta\Delta H_f$ values are rather small because these effects on the electron-transfer oxidation of DMAs and those on the deprotonation of $DMAs^{•+}$ are opposite, e.g., the electron-donating group favors the electron-transfer process but disfavors the deprotonation process of

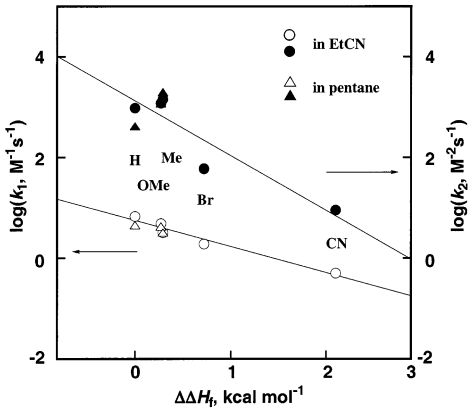

Figure 7. Plots of log k_1 and log k_2 versus $\Delta\Delta H_f$ for hydrogen transfer from DMAs to $PhCMe_2OO^•$ in O_2-saturated EtCN and pentane at 193 K. The $\Delta\Delta H_f$ value of DMA is taken as zero.

$DMAs^{•+}$.[40] Plots of log k_1 and log k_2 versus $\Delta\Delta H_f$ are shown in Figure 7, where linear correlations are obtained, supporting the one-step hydrogen atom transfer mechanism. Similar results are obtained from the DFT calculations (see Supporting Information, S2).[41]

Oxygen Transfer from Cumylperoxyl Radical to Triphenylphosphines and Sulfides. The decay rate of cumylperoxyl radical after cutting off the light is accelerated by the presence of triphenylphosphine as a result of an oxygen transfer from cumylperoxyl radical to triphenylphosphine. The oxygenated product was identified as triphenylphosphine oxide after the photoirradiation of the Bu^tOOBu^t-cumene-Ph_3P system (see Experimental Section). The pseudo-first-order rate constants for oxygen-transfer reactions from cumylperoxyl radicals to a series of *para*-substituted triphenylphosphines in EtCN at 193 K increase linearly with an increase in the concentrations of triphenylphosphines in propionitrile to give only the observed second-order rate constant (k_1) (see Supporting Information, S3). In pentane, however, the pseudo-first-order rate constants increase with an increase in the concentrations of triphenylphosphines to exhibit first-order dependence at low concentrations, changing to second-order dependence at high concentrations as observed in hydrogen-transfer reactions from DMAs to cumylperoxyl radicals (S4). The reason of such a difference in the kinetic order depending on solvents will be discussed in relation with the mechanism later. The k_1 and k_2 values for the oxygen-transfer reactions are summarized in Table 2 together with the one-electron oxidation potentials of triphenylphosphines (E^0_{ox}).

The dependence of log k_1 in EtCN on E^0_{ox} and that of log k_1 and log k_2 in pentane on E^0_{ox} are shown in Figure 8. In each case the log k_1 and log k_2 values are rather constant irrespective of E^0_{ox} and the k_1 values in a nonpolar solvent (pentane) are much larger than those in a polar solvent (EtCN). These trends are inconsistent with an electron-transfer mechanism, indicating that the oxygen transfer proceeds via a direct transfer of oxygen atom from cumylperoxyl radical to triphenylphosphines as shown in Scheme 2.

(39) The E^0_{ox} values were determined as the reversible oxidation potentials by the CV and SHACV.

(40) Such opposite effects may result in the bell-shaped nearly constant dependence of k_{obs} on E^0_{ox} in Figure 6. Similarly, the C−H bond dissociation energies of *para*-substituted toluene derivatives are reported to be hardly affected by the substitution, although the ionization potentials are sensitive to the ring substituents; see ref 31.

(41) Because the difference in $\Delta\Delta H_f$ values is small (<2 kcal mol^{-1}), the correlations in the plots of log k_1 and log k_2 versus $\Delta\Delta H_f$ are qualitative rather than quantitative.

Table 2. Oxidation Potentials (E^0_{ox}) and Rate Constants (k_1, k_2) for Oxygen Transfer from $PhCMe_2OO^•$ to Phosphines in O_2-Saturated EtCN and Pentane at 193 K

phosphine	E^0_{ox} (vs SCE,[a] V)	k_1[b] ($M^{-1}\,s^{-1}$)	k_2[b] ($M^{-2}\,s^{-1}$)
$(p\text{-}MeOC_6H_4)_3P$	0.80	*c* (1.3)[d]	*c*
$(p\text{-}MeC_6H_4)_3P$	0.97	2.0×10^2 (1.8)[d]	5.0×10^5
$(p\text{-}MeC_6H_4)Ph_2P$	1.02	1.2×10^2 (2.1)[d]	3.7×10^5
Ph_3P	1.06	1.0×10^2 (2.9)[d]	1.9×10^5
$(p\text{-}FC_6H_4)_3P$	1.17	8.4×10 (2.1)[d]	1.3×10^5
$(p\text{-}ClC_6H_4)_3P$	1.28	*c* (2.0)[d]	*c*
$EtPh_2P$	1.23	8.3×10	7.0×10^4
Et_2PhP	1.27	6.1×10	2.0×10^4
Me_2PhP	1.28	5.2×10	1.7×10^5
$MePh_2P$	1.30	8.0×10	1.1×10^5
$n\text{-}Pr_3P$	1.56	1.6×10	1.0×10^4

[a] Determined in MeCN. [b] Determined in pentane. [c] Not determined. [d] Values in parentheses are determined in EtCN.

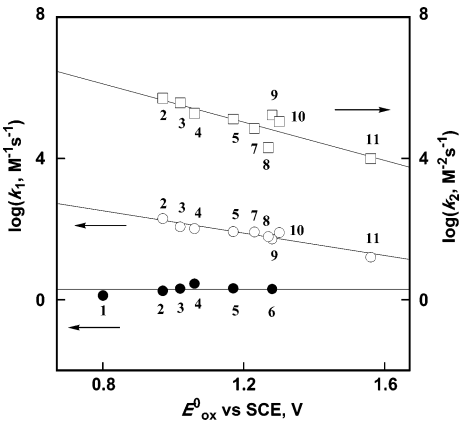

Figure 8. Plots of log k_1 and log k_2 versus E^0_{ox} of phosphines for oxygen transfer from $PhCMe_2OO^•$ to *para*-substituted R_3P's [$(p\text{-}MeOC_6H_4)_3P$ **1**, $(p\text{-}MeC_6H_4)_3P$ **2**, $(p\text{-}MeC_6H_4)Ph_2P$ **3**, Ph_3P **4**, $(p\text{-}FC_6H_4)_3P$ **5**, $(p\text{-}ClC_6H_4)_3P$ **6**, $EtPh_2P$ **7**, Et_2PhP **8**, Me_2PhP **9**, $MePh_2P$ **10**, and $n\text{-}Pr_3P$ **11**] in O_2-saturated EtCN (●) and pentane (○, □) at 193 K.

Scheme 2

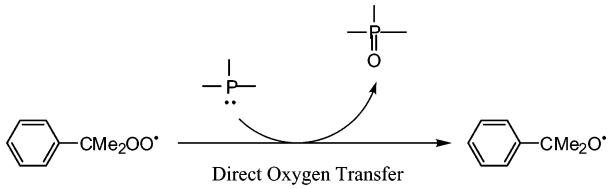

The rates of oxygen-transfer reactions of cumylperoxyl radical were also determined for the reactions with a variety of sulfides. The oxygen-transfer rates in EtCN were too slow to be determined accurately, and therefore they were determined only in pentane. The pseudo-first-order rate constants for the decay rates of cumylperoxyl radical in the presence of sulfides also exhibited first-order dependence with respect to the sulfide concentrations at low concentrations, changing to second-order dependence at high concentrations (S5). The k_1 and k_2 values for the oxygen-transfer reactions are summarized in Table 3 together with the one-electron oxidation potentials of sulfides (E^0_{ox}) (see Experimental Section).

The dependence of log k_1 and log k_2 for oxygen-transfer reactions from cumylperoxyl radical to sulfides on E^0_{ox} is shown in Figure 9, where log k_1 and log k_2 exhibit rather constant but somewhat scattered dependence on E^0_{ox}. In contrast to such scattered dependence of log k_1 and log k_2 on E^0_{ox} in Figure 9, they are much better correlated with the enthalpy change of the

Table 3. One-Electron Oxidation Potentials and Rate Constants (k_1, k_2) for Oxygen Transfer from $PhCMe_2OO^•$ to Sulfides in O_2-Saturated Pentane at 193 K

sulfide	E^0_{ox} (vs SCE,[a] V)	k_1[b] ($M^{-1}\,s^{-1}$)	k_2[b] ($M^{-2}\,s^{-1}$)
MeO-TA	1.13	1.4	1.3×10^2
Me-TA	1.24	1.6×10^{-1}	1.9
TA	1.34	3.5×10^{-1}	9.0×10^{-2}
Cl-TA	1.37	1.7	5.3
Me_2S	1.37	5.5×10^{-1}	5.0
Ph_2S	1.43	7.3×10^{-1}	8.4×10
Et_2S	1.57	3.9	6.1×10^2
$n\text{-}Pr_2S$	1.58	2.1	2.3×10
$t\text{-}Bu_2S$	1.59	1.1×10^{-1}	7.0×10^{-1}
$n\text{-}Bu_2S$	1.63	2.7	1.4×10^2

[a] Determined in MeCN. [b] Determined in pentane at 193 K.

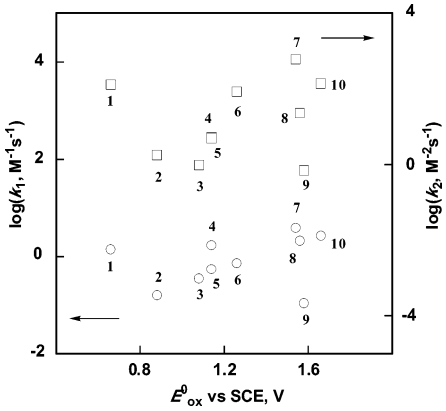

Figure 9. Plots of log k_1 and log k_2 versus E^0_{ox} of sulfides for oxygen transfer from $PhCMe_2OO^•$ to sulfides [MeO-TA **1**, Me-TA **2**, TA **3**, Cl-TA **4**, Me_2S **5**, Ph_2S **6**, Et_2S **7**, $n\text{-}Pr_2S$ **8**, $t\text{-}Bu_2S$ **9**, and $n\text{-}Bu_2S$ **10**] in O_2-saturated pentane at 193 K.

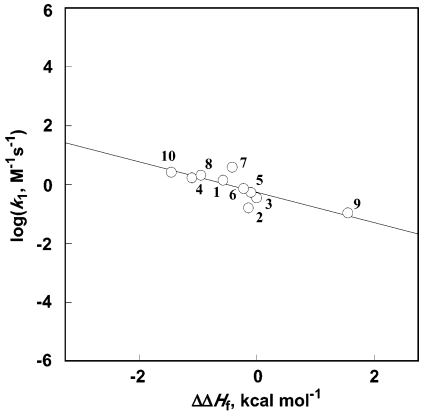

Figure 10. Plot of log k_1 versus $\Delta\Delta H_f$ for oxygen transfer from $PhCMe_2OO^•$ to sulfides [MeO-TA **1**, Me-TA **2**, TA **3**, Cl-TA **4**, Me_2S **5**, Ph_2S **6**, Et_2S **7**, $n\text{-}Pr_2S$ **8**, $t\text{-}Bu_2S$ **9**, and $n\text{-}Bu_2S$ **10**] in O_2-saturated pentane at 193 K. The $\Delta\Delta H_f$ value of TA is taken as zero.

oxygen transfer reactions ($\Delta\Delta H_f$) as shown in Figure 10, where the $\Delta\Delta H_f$ values are calculated as the difference in heat of formation between sulfides and the corresponding sulfoxides by using the PM3 semiempirical MO method (see Experimental Section). This indicates that oxygen-transfer reactions from cumylperoxyl radicals to sulfides proceed via a direct oxygen atom transfer rather than via electron transfer as shown in Scheme 3. The substituent effects of electron-donating or electron-withdrawing groups of thioanisole on the $\Delta\Delta H_f$ values in Figure 10 are small as the case of DMAs in Figure 7 (vide

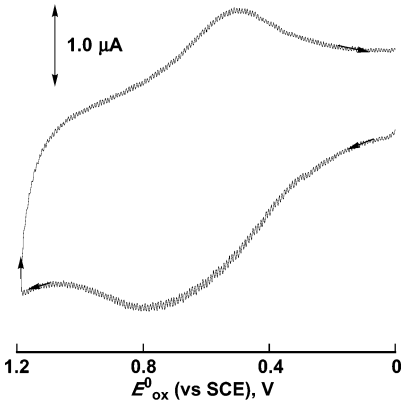

Figure 11. Cyclic voltammogram of $PhCMe_2OO^-$ formed in the reaction of $PhCMe_2OOH$ (2.0 mM) with *n*-Bu_4NOH (2.0 mM) in deaerated EtCN containing 0.1 M $TBAPF_6$. Working electrode, Pt; counter electrode, Pt; reference electrode, $Ag/AgNO_3$; scan rate, 500 mV s^{-1}.

Scheme 3

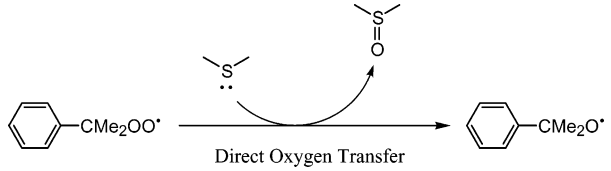

supra). In the case of thioanisoles (TAs) as well, the substituent effects on the electron-transfer oxidation of TAs and those on the O^- affinity of $TAs^{\bullet+}$ are opposite, e.g., the electron donating group favors the electron-transfer process but disfavors the O^- binding of $TAs^{\bullet+}$.

Because some substrates have relatively low one-electron oxidation potentials, it may be possible that an electron-transfer step plays an important role in some hydrogen- and oxygen-transfer reactions examined in this study. Thus, the possible contribution of an electron-transfer step can be further examined by comparing the rate constants determined for electron-transfer reactions from ferrocene derivatives to cumylperoxyl radical and the effects of metal ions on the electron-transfer rates with those for the hydrogen-transfer reactions from DMAs to cumylperoxyl radical (vide infra).

Electron Transfer from Ferrocene Derivatives to Cumylperoxyl Radical. Alkylperoxyl radicals ($ROO^{\bullet}$) are regarded as rather strong one-electron oxidants judging from the positive one-electron reduction potentials (E^0_{red} vs NHE = 0.6−1.2 V depending on R).[42,43] There have been reports on electron-transfer reactions from a variety of electron donors to alkylperoxyl radicals.[44−46] The direct determination of the E^0_{red} value of cumylperoxyl radical was performed by the cyclic voltammogram of $PhCMe_2OO^-$ produced by the reaction of $PhCMe_2OOH$ with Me_4NOH (Figure 11).

The E^0_{red} value is determined as 0.65 V versus SCE. Thus, electron transfer from ferrocene (E^0_{ox} vs SCE = 0.37 V)[47] to cumylperoxyl radical is energetically feasible. In fact, the decay rate of cumylperoxyl radical was significantly enhanced by the presence of ferrocene derivatives. The decay rate in the presence of ferrocene derivatives also obeyed pseudo-first-order kinetics and the pseudo-first-order rate constants increase linearly with increasing the concentrations of ferrocene derivatives (S6). The observed second-order rate constants of the electron-transfer reactions (k_{et}) are summarized in Table 4 together with the free energy change of the electron transfer (ΔG^0_{et}), which is obtained from the E^0_{ox} values of ferrocene derivatives[47] and the E^0_{red} value of cumylperoxyl radical. The k_{et} value increases with decreasing the ΔG^0_{et} value, as expected for the electron transfer from ferrocene derivatives to cumylperoxyl radical.

Table 4. Free Energy Changes (ΔG^0_{et}), Rate Constants (k_{et}), and Reorganization Energies (λ_{ex}) for Electron Transfer from Ferrocene Derivatives to $PhCMe_2OO^{\bullet}$ in O_2-Saturated EtCN at 193 K

ferrocene derivative	ΔG^0_{et}[a] (eV)	k_{et}[b] (M^{-1} s^{-1})	λ_{ex} (kcal mol^{-1})
$Fe(C_5Me_5)_2$	−0.73	9.1×10	189
$Fe(C_5H_4Bu^n)_2$	0.40	3.2	184
$Fe(C_5H_4Me)_2$	0.39	3.0	186
$Fe(C_5H_5)(C_5H_4Bu^n)$	0.34	0.8	*c*
$Fe(C_5H_5)_2$	0.28	2.0×10^{-2}	185

[a] Determined in MeCN. [b] Determined in EtCN. [c] Not determined because no λ_{ex}' value of the ferrocene derivative is obtained.

The self-exchange rate constants (k_{ex}) of $PhCMe_2OO^{\bullet}$/$PhCMe_2OO^-$ can be determined from the electron-transfer rate constant (k_{et}) and the self-exchange rate constants (k_{ex}') of ferrocene derivative/ferricenium derivative[48] by using the Marcus eqs 2 and 3:[19]

$$k_{ex} = \frac{k_{et}^{\,2}}{k_{ex}' K_{et} f} \tag{2}$$

$$\ln f = \frac{(\ln K_{et})^2}{4 \ln\left(\frac{k_{ex} k_{ex}'}{Z^2}\right)} \tag{3}$$

where K_{et} is the equilibrium constant for electron transfer, f is a correction factor (generally close to 1), and Z is the collision frequency, taken as 1.0×10^{11} M^{-1} s^{-1}. The K_{et} values are obtained from the ΔG^0_{et} values by using eq 4. The k_{ex} values of $PhCMe_2OO^{\bullet}$/$PhCMe_2OO^-$ are converted to the reorganization energy (λ_{ex}) for the self-exchange electron-transfer reaction between $PhCMe_2OO^{\bullet}$ and $PhCMe_2OO^-$ using eq 5.

$$K_{et} = \exp\left(\frac{-\Delta G^0_{et}}{RT}\right) \tag{4}$$

$$\lambda_{ex} = 4RT(\ln Z - \ln k_{ex}) \tag{5}$$

The λ_{ex} values thus determined are also listed in Table 4. The large λ_{ex} value in Table 2 indicates that a significant outer- and inner-reorganization is required for electron-transfer reactions of cumylperoxyl radical as is reported in the case of electron-transfer reactions of oxygen.[49,50]

(42) Jonsson, M. *J. Phys. Chem.* **1996**, *100*, 6814.
(43) Merenyi, G.; Lind, J.; Engman, L. *J. Chem. Soc., Perkin Trans. 2* **1994**, 2551.
(44) (a) Alfassi, Z. B.; Mosseri, S.; Neta, P. *J. Phys. Chem.* **1989**, *93*, 1380. (b) Khaikin, G. I.; Alfassi, Z. B.; Neta, P. *J. Phys. Chem.* **1995**, *99*, 16722.
(45) (a) Khaikin, G. I.; Alfassi, Z. B.; Huie, R. E.; Neta, P. *J. Phys. Chem.* **1996**, *100*, 7072. (b) Neta, P.; Huie, R. E.; Ross, A. B. *J. Phys. Chem. Ref. Data* **1990**, *19*, 413.
(46) Workentin, M. S.; Maran, F.; Wayner, D. D. M. *J. Am. Chem. Soc.* **1995**, *117*, 2120.
(47) Fukuzumi, S.; Mochizuki, S.; Tanaka, T. *Inorg. Chem.* **1989**, *28*, 2459.
(48) Yang, E. S.; Chan, M.-S.; Wahl, A. C. *J. Phys. Chem.* **1980**, *84*, 3094.
(49) Lind, J.; Shen, X.; Merényi, G.; Jonsson, B. Ö. *J. Am. Chem. Soc.* **1989**, *111*, 7654.

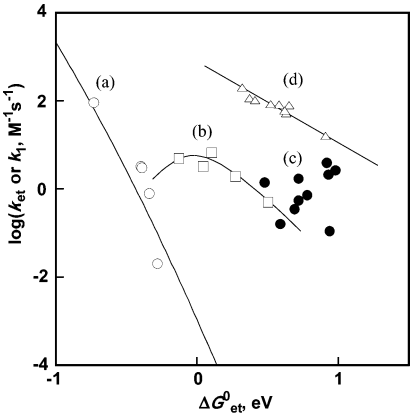

Figure 12. Dependence of log k_{et} and log k_1 on ΔG^0_{et} for (a) electron transfer from ferrocene derivatives to $PhCMe_2OO^•$, (b) hydrogen transfer from DMAs to $PhCMe_2OO^•$, (c) oxygen transfer from $PhCMe_2OO^•$ to phosphines, and (d) oxygen transfer from $PhCMe_2OO^•$ to sulfides in O_2-saturated EtCN and pentane at 193 K.

The dependence of log k_{et} on ΔG^0_{et} is given by eq 6, which

$$\log k_{et} = \log Z - \frac{\left(\frac{\lambda}{4}\right)\left(1 + \frac{\Delta G^0_{et}}{\lambda}\right)^2}{2.3RT} \qquad (6)$$

is derived from eqs 2−4. The reorganization energy of electron transfer (λ) corresponds to the average of each component, λ_{ex} for the electron self-exchange of $PhCMe_2OO^•/PhCMe_2OO^-$ and λ_{ex}' of ferrocene derivative/ferricenium ion derivative. The fit of the curves to the Marcus theory of adiabatic outer-sphere electron transfer (eq 6) indicates that the rate variations at a given ΔG^0_{et} value arise from the difference in the λ value given in Figure 12 and not from the nonadiabaticity.[51]

The log k_1 values for hydrogen- and oxygen-transfer reactions of cumylperoxyl radical with DMAs and those for oxygen-transfer reactions with triphenylphosphines and sulfides are plotted in Figure 12 for comparison. The log k_1 values in each case are much larger than the corresponding k_{et} values at the same ΔG^0_{et} values, indicating also that the hydrogen- and oxygen-transfer reactions proceed via a one-step hydrogen atom or an oxygen atom transfer rather than the rate-determining electron transfer as shown in Schemes 1, 2, and 3, respectively.

The rate of electron transfer from ferrocene to cumylperoxyl radical is enhanced significantly by the presence of metal ions such as $Sc(OTf)_3$ and $Y(OTf)_3$. The k_{et} values increase with increasing the metal ion concentration as shown in Figure 13a, whereas Mg^{2+} shows a slight acceleration effect on the rate of electron transfer from ferrocene to cumylperoxyl radical (see Supporting Information S7). The acceleration effect of metal ions can be ascribed to the binding of the $PhCMe_2OO^-$ to the metal ions, which results in a decrease in the free energy of the electron transfer as shown in Scheme 4.[52,53]

In contrast to the case of electron-transfer reactions of cumylperoxyl radical (Figure 13a), there was little effect of

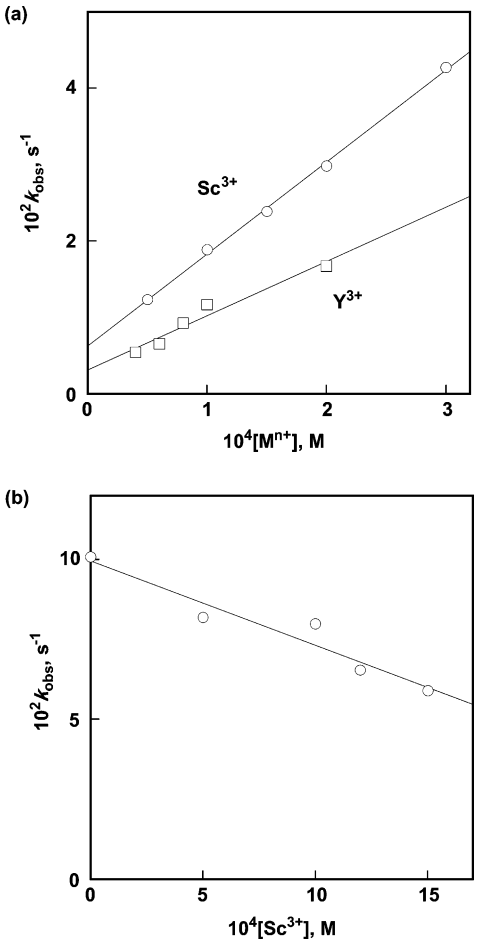

Figure 13. (a) Plots of k_{obs} versus $[M^{n+}]$ ($M^{n+} = Sc^{3+}$ and Y^{3+}) for electron transfer from $Fe(C_5H_5)_2$ (2.0×10^{-3} M) to $PhCMe_2OO^•$ in the presence of M^{n+} in O_2-saturated EtCN at 193 K. (b) Plot of k_{obs} versus $[Sc^{3+}]$ for hydrogen transfer from DMA (1.0×10^{-2} M) to $PhCMe_2OO^•$ in the presence of Sc^{3+} in O_2-saturated EtCN at 193 K.

Scheme 4

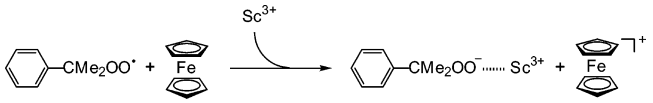

$Sc(OTf)_3$ on the rate of hydrogen transfer from DMA to cumylperoxyl radical in EtCN as shown in Figure 13b.[53,54] This indicates that there is no contribution of an electron-transfer step from DMA to cumylperoxyl radical in the hydrogen-transfer reaction.

Hydrogen- and Oxygen-Transfer Reactions via Charge-Transfer Complexes. Although no complete transfer of an electron is involved in the hydrogen-transfer reaction from DMAs to cumylperoxyl radical (vide supra), the first-order and second-order dependence of k_{obs} with respect to the DMAs concentrations suggests the involvement of charge-transfer

(50) (a) McDowell, M. S.; Espenson, J. H.; Bakač, A. *Inorg. Chem.* **1984**, *23*, 2232. (b) Zahir, K.; Espenson, J. H.; Bakač, A. *J. Am. Chem. Soc.* **1988**, *110*, 5059.

(51) For the different λ_{ex}' values, see ref 50.

(52) There was no effect of $Sc(OTf)_3$ on the oxidation potential of ferrocene. There was no effect of $Sc(OTf)_3$ on the ESR spectrum of $PhCMe_2OO^•$, either. Thus, the complexation of RO_2^- with $Sc(OTf)_3$, which is coupled with the electron transfer, is responsible for the acceleration effect of $Sc(OTf)_3$ on the electron transfer. For the detailed discussion on metal ion-promoted electron-transfer reactions, see ref 53.

(53) (a) Fukuzumi, S. In *Electron Transfer in Chemistry*; Balzani, V., Ed.; Wiley-VCH: Weinheim, 2001; Vol. 4, pp 3−67. (b) Fukuzumi, S. *Bull. Chem. Soc. Jpn.* **1997**, *70*, 1. (c) Fukuzumi, S. *Org. Biomol. Chem.* **2003**, *1*, 609. (d) Fukuzumi, S.; Itoh, S. In *Advances in Photochemistry*; Neckers, D. C., Volman, D. H., von Bünau, G., Eds.; Wiley: New York, 1998; Vol. 25, pp 107−172. (e) Fukuzumi, S.; Okamoto, K.; Imahori, H. *Angew. Chem., Int. Ed.* **2002**, *41*, 620. (f) Fukuzumi, S.; Okamoto, K.; Yoshida, Y.; Imahori, H.; Araki, Y.; Ito, O. *J. Am. Chem. Soc.* **2003**, *125*, 1007.

(54) In the presence of $Sc(OTf)_3$, the rate constant decreases slightly with increase in the $Sc(OTf)_3$ concentration (Figure 13b), probably as a result of the complex formation of $Sc(OTf)_3$ with DMA.

Scheme 5

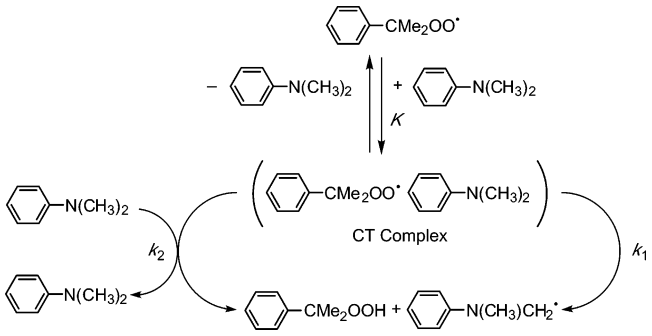

complexes formed between DMAs and cumylperoxyl radical as shown in Scheme 5. The formation of charge-transfer complexes between DMAs and a variety of electron donors has been well-documented in the literature.[55,56] Since cumylperoxyl radical is a strong electron acceptor judging from the highly positive E^0_{red} value (0.65 V vs SCE) as compared to other electron acceptors that are known to form the CT complexes with DMAs, cumylperoxyl radical may form CT complexes with DMAs. The first-order and second-order dependence of k_{obs} on [DMAs] may thereby be ascribed to the intracomplex hydrogen transfer in the CT complex (first-order with respect to [DMAs]) and the bimolecular hydrogen transfer from DMA to the CT complex (second-order with respect to [DMAs]), respectively.[57] The bimolecular hydrogen transfer from DMA to the CT complex may proceed via a 2:1 CT complex formed between DMA and cumylperoxyl radical. In the case of oxygen-transfer reactions from cumylperoxyl radical to triphenylphosphines and sulfides as well, the observed first-order and second-order dependence of k_{obs} on the substrate concentration indicates that CT complexes formed between cumylperoxyl radical and substrates act as reactive intermediates for the one-step oxygen atom transfer reactions. In nonpolar solvents such as pentane, the CT complex may be more stabilized by forming a 2:1 CT complex between substrates and cumylperoxyl radical,[58] when the second-order dependence of k_{obs} on substrate concentration becomes more important as compared with the case in a polar solvent (EtCN) as reported for brominations of electron donors in nonpolar solvents.[37] Although it is difficult to observe the CT spectra of the DMA- and TA-cumylperoxyl radical complexes because of the instability of the radical complexes, a decrease in the *g* value of cumylperoxyl radical is observed with increasing the DMA and TA concentrations (see Supporting Information S8).[59] This indicates the formation of the CT complex of cumylperoxyl radical with DMA and TA.[60]

Acknowledgment. This work was partially supported by Grants-in-Aid for Scientific Research on Priority Area (nos. 13440216 and 14045249) from the Ministry of Education, Culture, Sports, Science and Technology, Japan. We thank Dr. Y. Goto for supplying us DMAs-$(CD_3)_2$.

Supporting Information Available: Plots of k_{obs} versus concentrations of *N*,*N*-dimethylanilines for hydrogen transfer from DMAs to $PhCMe_2OO^•$ in EtCN (S1), plots of log k_1 and log k_2 versus $\Delta\Delta H_f$ (S2), plots of k_{obs} versus concentrations of triphenylphosphine derivatives for oxygen transfer from $PhCMe_2OO^•$ to triphenylphosphine derivatives in EtCN (S3), plots of k_{obs} versus concentrations of triphenylphosphine derivatives for oxygen transfer from $PhCMe_2OO^•$ to triphenylphosphine derivatives in pentane (S4), plots of k_{obs} versus concentrations of TAs for oxygen transfer from $PhCMe_2OO^•$ to TAs in pentane (S5), plots of k_{obs} versus concentrations of ferrocene derivatives for electron transfer from ferrocene derivatives to $PhCMe_2OO^•$ (S6), plot of k_{obs} versus $[Mg^{2+}]$ for electron transfer from $Fe(C_5H_5)_2$ to $PhCMe_2OO^•$ in the presence of Mg^{2+} (S7), and plot of *g* value of $PhCMe_2OO^•$ versus concentrations of DMA and TA (S8). This material is available free of charge via the Internet at http://pubs.acs.org.

JA035156O

(55) Mulliken, R. S.; Person, W. B. *Molecular Complexes*, a Lecture and Reprint Volume; Wiley-Interscience: New York, 1969.
(56) Zweig, A.; Lancaster, J. E.; Neglia, M. T.; Jura, W. H. *J. Am. Chem. Soc.* **1964**, *86*, 4130.
(57) According to Scheme 5, $k_{obs} = k_1[PhCMe_2OO^• DMA] + k_2[PhCMe_2OO^• DMA][DMA]$, where $[PhCMe_2OO^• DMA] = K[PhCMe_2OO^•][DMA]$ and thus, $k_{obs} = k_1K[PhCMe_2OO^•][DMA] + k_2K[PhCMe_2OO^•][DMA]^2$.
(58) The addition interaction of a substrate to a 1:1 CT complex in nonpolar solvents may enhance the CT interaction as reported in ref 37.
(59) The larger *g* value of cumylperoxyl radical than the free spin value (2.0023) is ascribed to the spin−orbit coupling interaction on oxygen atom, which has a large spin−orbit coupling constant. The charge-transfer interaction of cumylperoxyl radical with electron donors results in a decrease in the spin density on oxygen, which causes the decrease in the *g* value (S8).
(60) For the CT complex formation of cumylperoxyl radical with pyridine, see: Fukuzumi, S.; Ono, Y. *Bull. Chem. Soc. Jpn.* **1977**, *50*, 2063.